Detecting red blotch disease in grape leaves using hyperspectral imaging

Mehrube Mehrubeoglu*[a], Keith Orlebeck[b], Michael J. Zemlan[b], and Wesley Autran[b]
[a]Texas A&M University-Corpus Christi, 6300 Ocean Drive, Corpus Christi, TX 78412-5797, USA;
[b]Surface Optics Corporation, 11555 Rancho Bernardo Rd., San Diego, CA 92127, USA

ABSTRACT

Red blotch disease is a viral disease that affects grapevines. Symptoms appear as irregular blotches on grape leaves with pink and red veins on the underside of the leaves. Red blotch disease causes a reduction in the accumulation of sugar in grapevines affecting the quality of grapes and resulting in delayed harvest. Detecting and monitoring this disease early is important for grapevine management. This work focuses on the use of hyperspectral imaging for detection and mapping red blotch disease in grape leaves. Grape leaves with known red blotch disease have been imaged with a portable hyperspectral imaging system both on and off the vine to investigate the spectral signature of red blotch disease as well as to identify the diseased areas on the leaves. Modified reflectance calculated at spectral bands corresponding to 566 nm (green) and 628 nm (red), and modified reflectance ratios computed at two sets of bands (566 nm / 628 nm, 680 nm / 738 nm) were selected as effective features to differentiate red blotch from healthy-looking and dry leaf. These two modified reflectance and two ratios of modified reflectance values were then used to train the support vector machine classifier in a supervised learning scheme. Once the SVM classifier was defined, two-class classification was achieved for grape leaf hyperspectral images. Identification of the red blotch disease on grape leaves as well as mapping different stages of the disease using hyperspectral imaging are presented in this paper.
Keywords: Hyperspectral imaging, red blotch disease, SVM classifier, image processing, spectral and spatial characterization, grapevine management

1. INTRODUCTION

Red blotch disease (RBD) is a viral disease that affects grapevines. Red blotch disease shows similar symptoms to leafroll disease, and is transmitted through pests and grafting[1,2]. The primary symptoms are leaves turning red at the base of the shoots with pink and red veins on the underside of the leaves. Red blotch disease causes a reduction in the accumulation of sugar in grapevines affecting the quality of grapes and resulting in delayed harvest[3]. There would be great value for viticulturists and grape growers to detect this disease, and watch its progression for disease management. This paper focuses on hyperspectral imaging of red blotch disease in grape leaves on and off the vine using a portable hyperspectral imaging system. The final result is mapping the red blotch diseased areas on the grape leaf.

Inspecting and monitoring grapevine health through grapes and grape leaves have attracted the attention of viticulturists and technologists alike. Rapaport *et al.* report investigating water stress in grape leaves using hyperspectral imaging and partial least squares regression (PLS-R) as a more affordable and faster alternative tool to physiological measurements[4]. The authors found 530–550 nm and around 1500 nm to be useful bands for separating pigment changes and water content in grape leaves[4]. Fernandes *et al.* utilized the same methods, namely hyperspectral imaging and partial least squares, to classify four different clones of grape leaves[5]. The authors' research revealed second derivative of the normalized spectra in the range 634–759 nm produced above 97.8% to 100% classification rates using the PLS classifier. In an earlier paper, Lenk *et al.* incorporated multispectral fluorescence and reflectance imaging at the leaf level to investigate these two technologies' potential applications[6].

In this paper red blotch disease is separated from green leaf, dry leaf and background under a supervised support vector machine (SVM) classification scheme. SVM is a popular classifier that optimizes margins and decision boundaries between two classes[7,8]. Gualtieri and Chettri applied SVM to hyperspectral data cubes to differentiate corn and soy

*ruby.mehrubeoglu@tamucc.edu; phone 1 361 825-3378; fax 1 222 555-876

Algorithms and Technologies for Multispectral, Hyperspectral, and Ultraspectral Imagery XXII
edited by Miguel Velez-Reyes, David W. Messinger, Proc. of SPIE Vol. 9840, 98400D
 · doi: 10.1117/12.2223814

spectra from AVIRIS[9]. The authors compared the results of SVM to minimum-Euclidean distance method and demonstrated higher percent accuracy of classification with SVM. In their review paper on image processing techniques for detecting, quantifying and classifying plant diseases, Garcia and Barbedo summarized multiple research groups' work that utilized SVM for both two-class and multi-class classification[10]. In our paper, SVM is used as a binary or two-class classifier where RBD is treated as Class 1, and green leaf, dry leaf, and background are collectively treated as Class 2.

2. METHODS

2.1 Samples and Data Acquisition

Grape leaves with known red blotch disease were imaged with SOC710-VP® hyperspectral imager (Surface Optics Corp., San Diego, CA, USA) calibrated between 400 and 1000 nm (Figure 1). Grape leaves were imaged on the vine, immediately after having been picked off the vine (Figure 1), and after returning to the SOC labs (Figure 2). Off-the vine hyperspectral imaging was achieved by placing the leaves on a gray reference panel, which constituted the background. Figure 3 shows grape leaves at different stages of red blotch disease. The imager is composed of 520 lines, 696 samples and 128 bands[11].

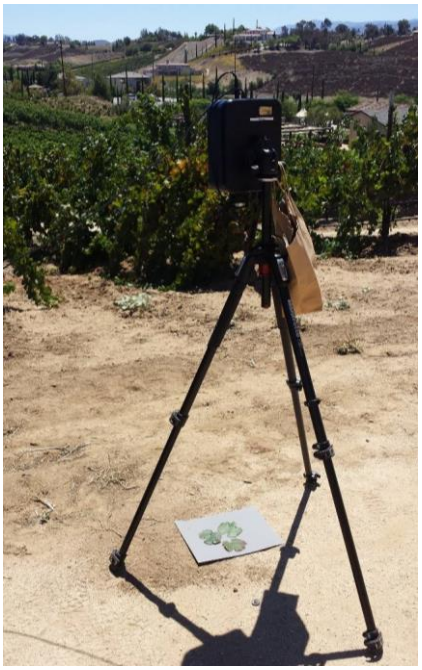

Figure 1. Portable hyperspectral imaging system (SOC710-VP®) and imaging off-the-vine leaves in the field.

(a) **(b)** **(c)**

Figure 2. Color images of red blotch diseased grape leaves obtained from the hyperspectral data cube acquired (a) on the vine, (b) immediately after the grape leaf was detached from the vine stalk, and (c) in the laboratory. (Southern California, 14 July 2015).

Figure 3. Red blotch disease at different stages.

2.2 Hyperspectral Data Processing and Analysis

For this project, the feature selection process involved identifying a combination of wavebands at which the modified reflectance (see below) or the ratio of modified reflectance values differentiate red blotch from the rest of the image. Figure 4 summarizes the data processing and analysis chain.

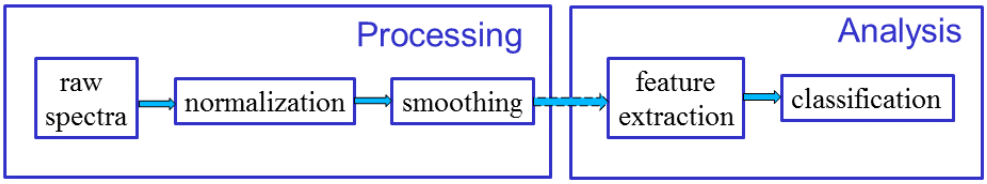

Figure 4. Hyperspectral data processing and analysis chain.

The acquired images were first normalized against the gray panel image for on-vine and off-vine leaf imaging, and for leaves brought back to the lab. The normalization process involves dividing the grapevine hyperspectral image by the gray reference panel image voxel-by-voxel as described in a previous paper[12].

$$I_N(i,j,k) = I(i,j,k) / (I_R(i,j,k), \text{ for } i=1,2,3,\ldots,M,\ j=1,2,3,\ldots,N,\ k=1,2,3,\ldots,Z, \quad (1)$$

where i refers to the line number, j represents the sample number, and k is the band number in the hyperspectral data cube. The imager is represented by 696 X 520 pixels such that M = 696, N = 520, with Z = 128 bands. $I(i,j,k)$ represents the raw hyperspectral data value at voxel (i,j,k), and $I_R(i,j,k)$ is the reference panel data value at corresponding coordinates. Finally $I_N(i,j,k)$ is the normalized data value. We note that the hyperspectral camera automatically subtracts a dark image from any acquired hyperspectral data cube such that I and I_R are resultant dark image-removed response of the camera. We call the result of the normalization process thus described modified reflectance due to the fact that the reference panel from which reference images are acquired is a uniform gray panel with approximately 18% reflectance in the captured spectral range as opposed to nearly perfect Lambertian reflectance targets typically used to compute reflectance. Modified reflectance of a given material is, therefore, expected to be higher than the reflectance obtained with 100% reflective materials according to Eq. (1).

Normalization is followed by smoothing, applied in the spectral dimension using a 5x1 averaging window[12]:

$$I_{NS}(i,j,k) = \frac{1}{5}\sum_{k-2}^{k+2} I_N(i,j,k), \ \forall\ i \in [1,695],\ j \in [1,520],\ k \in [3,126], \quad (2)$$

where $I_{NS}(i,j,k)$ represents the spectrally smoothed normalized hyperspectral voxel value at coordinates (i,j,k).

Once effective features are identified, classification is achieved via a SVM classifier as described in the next section.

3. DATA AND RESULTS

3.1 Spectral and Spatial Representation of Grape Leaves

Figure 5 shows sample spectra from different areas on the grape leaf of Figure 2 (b) selected and labeled by the user to represent green leaf and red blotch areas. Figure 5 depicts modified reflectance spectra of red blotch disease, green leaf and reference panel. In addition, spectra originally thought to be from red blotch disease but were then identified as 'sunburn' or dry leaf are represented. In the spatial domain, the modified reflectance image is calculated by dividing the hyperspectral leaf image by the reference image as formulated by Eq. (1). In addition, an area named 'sunburn' demonstrates distinct spectral signatures separating its spectral response from that of red blotch disease. This area represents similar discoloration as the red blotch disease; however, upon closer inspection, unlike red blotch diseased areas, this area appears to be colored by dehydrated spots or perhaps dead leaf with no chlorophyll content. This area must be further confirmed or alternately labeled by a viticulturist expert.

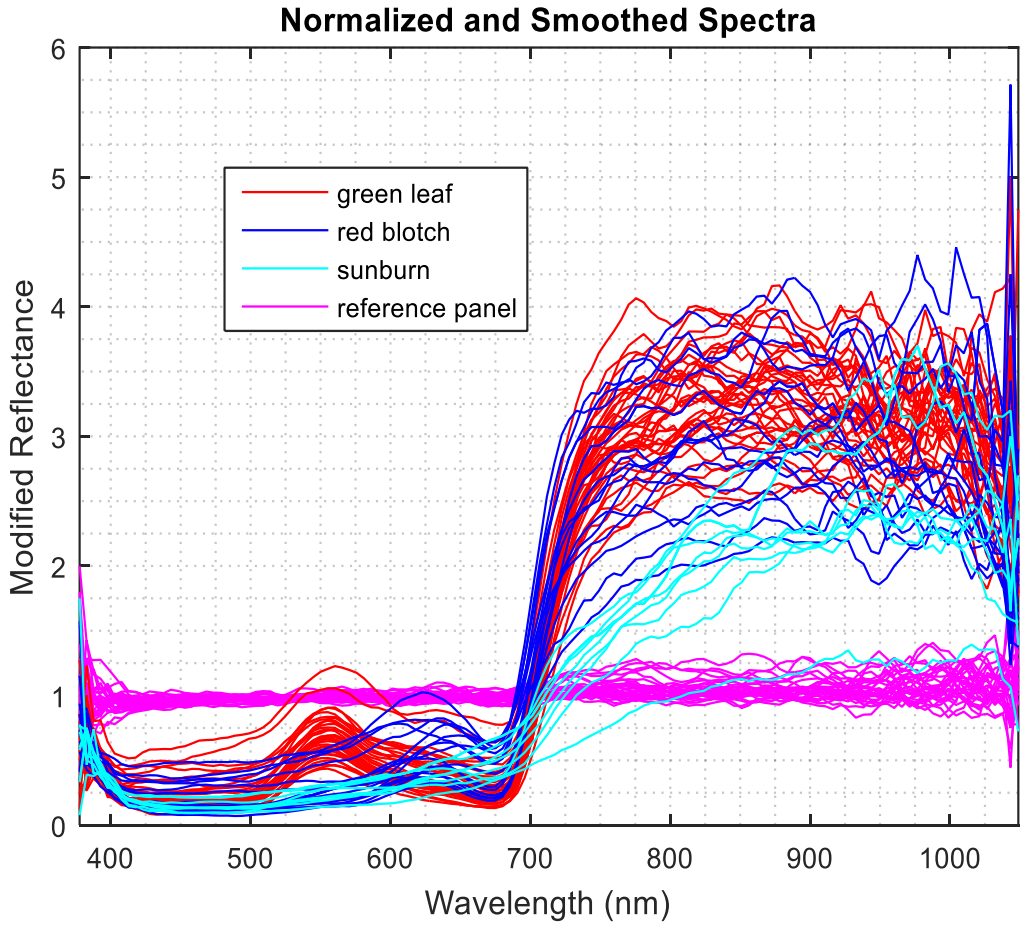

Figure 5. Modified Reflectance Spectra.

Visual inspection of spectra in Figure 5 reveals distinct spectral peaks, valleys as well as gradients between spectral wavebands for each of the regions of interest. Based on this visual assessment, spatial representation of grape leaves at different wavebands and waveband ratios are demonstrated in Figure 6. Spatial images of the grape leaves show the distinction among various regions of the leaf as well as the background.

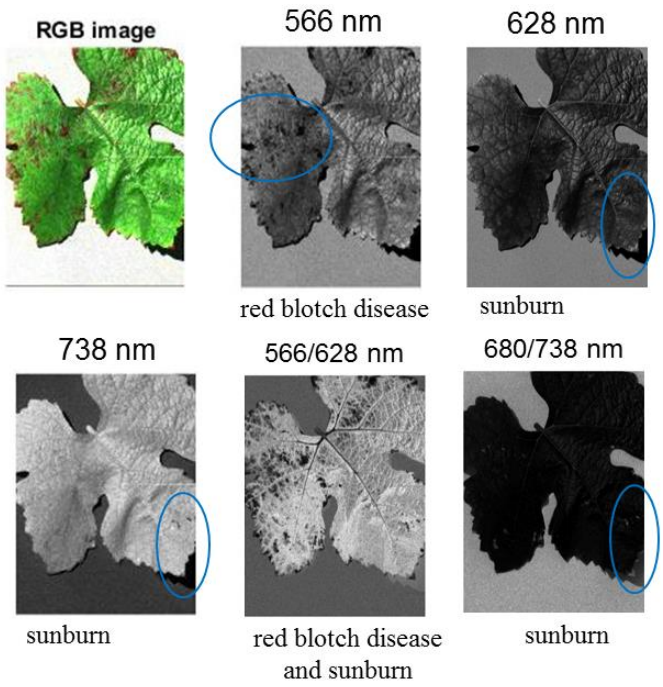

Figure 6. Spatial representation of grape leaf at various wavebands and waveband ratios highlighting different aspects of the leaf.

3.2 Feature Extraction and Classification

Table 1 summarizes bands at whose modified reflectance or ratio of modified reflectance values were selected as effective features. Based on the analysis described in the previous section, modified reflectance based on spectral bands associated with 566 nm and 628 nm with modified reflectance ratios based on band 566 nm and 628 nm, as well as 680 nm and 738 nm, were selected as features differentiating red blotch diseases from the rest of the scene. The modified reflectance based on these two bands and two band ratios were then used to train the SVM classifier in the supervised learning scheme.

Table 1. Wavebands, and associated modified reflectance values and ratios selected as effective features

WAVEBANDS (nm)	FEATURES (Modified Reflectance or Modified Reflectance Ratio)* (nu)
566	R_{566}
628	R_{628}
680	R_{566}/R_{628}
738	R_{680}/R_{738}

*R_x – Modified Reflectance; R_x/R_y – Modified Reflectance Ratio

For the training set, first normalized then smoothed spectra of Figure 5 extracted from the hyperspectral leaf image represented in Figure 2 (b) were used as labelled data. Red blotch diseased leaf spectra were labeled as Class 1. All other spectra (green leaf, background (gray reference panel) and sunburnt (dry) areas) were identified as Class 2 for the purpose of the binary SVM classifier. A quadratic kernel was used for classification programmed using MATLAB 2014

procedures. Two-class mapping of grape leaf images identifying RBD was achieved using the same training set of labelled spectra described above.

Figure 7 through 9 demonstrate the detection of red blotch disease on grape leaves on and off the vine and at various stages of the disease. Red blotch is clearly identifiable by the binary classification scheme in all the grape leaf hyperspectral images presented.

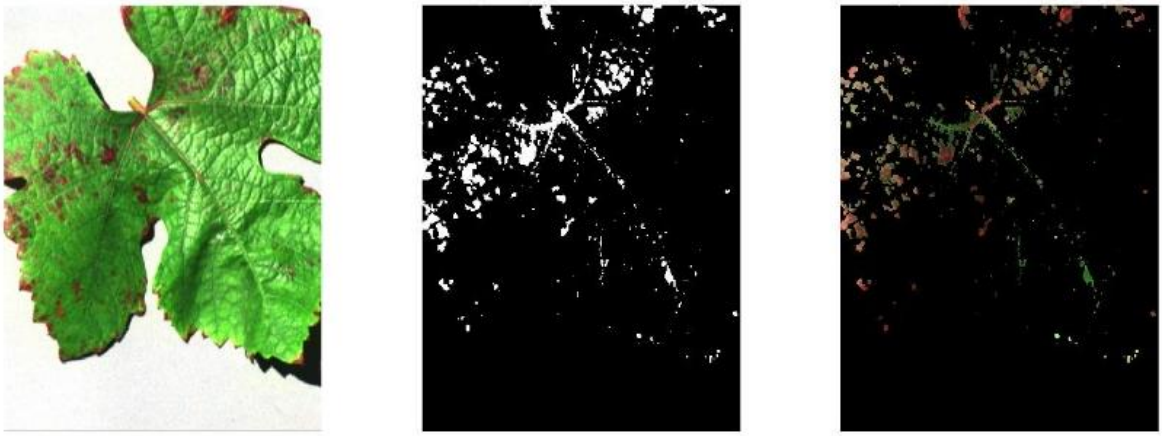

(a) (b) (c)

Figure 7. Detection of red blotch disease in the grape leaf of 2(b) acquired in the field after the leaf was removed from the vine. (a) Color representation of the grape leaf with red blotch disease; (b) mask of red blotch diseased areas on the leaf; (c) Color image of diseased areas on the leaf. (Data acquired in the field immediately after leaf was detached from the vine, 14 July 2015)

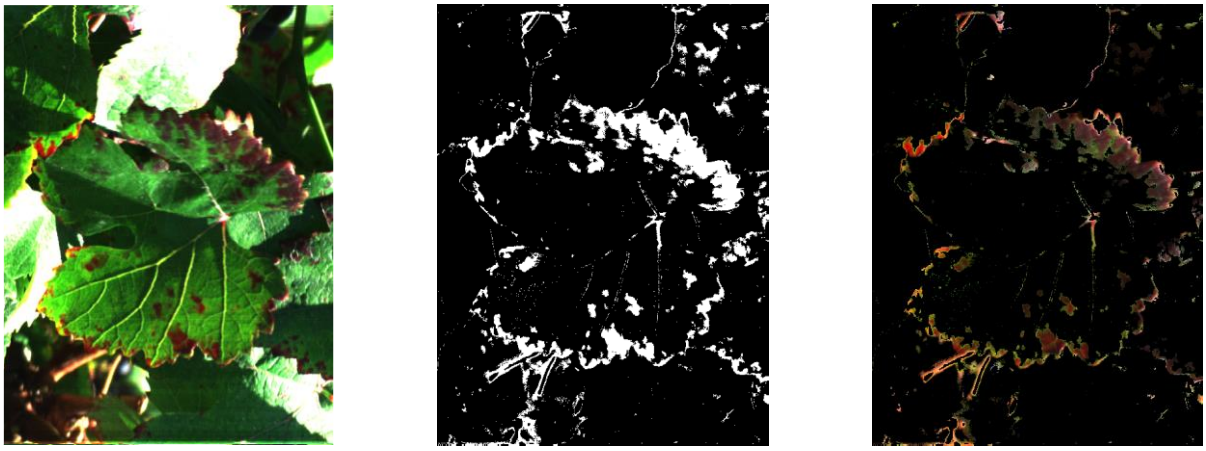

Figure 8. Detection of red blotch disease on grape leaves on the vine. (a) Color image of grape leaves with RBD; (b) mask of red blotched diseased areas; (c) color image of RBD on the leaves. (Data acquired on the vine, 23 July 2015)

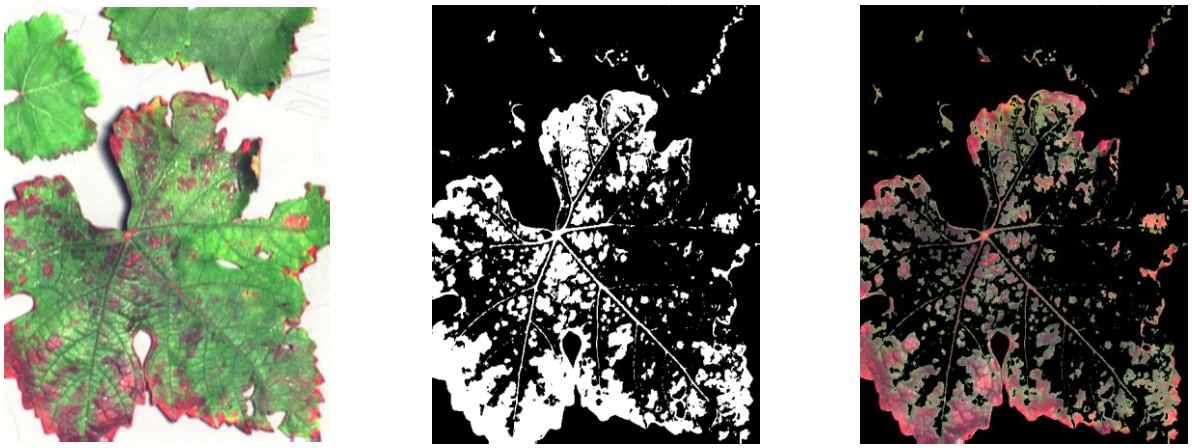

Figure 9. (a) Color image of three grape leaves at different states of red blotch disease; (b) mask of red blotch diseased areas; (c) color image of identified RBD on the leaf. (Data acquired at SOC labs, 23 July 2015)

Figures 7-9 show the mapping of the red blotch disease on the grape leaves in ascending order of advancement of the disease demonstrated in different leaves. In Figure 7, the disease appears to have started at the root of the stalk and spread along the left and right sides of the top of the leaf covering less than 25% of the leaf surface. In Figure 8, the disease appears to have spread around the periphery of the leaf including other minor veins. In Figure 9, RBD is visible on well over 50% of the leaf surface, including leaf area and veins. This methodology can thus be used to identify and then quantify red blotch disease on grape leaves as part of a potential disease monitoring and management strategy.

4. DISCUSSION

The 2D RBD maps on the grape leaf surface depicted in Figures 7-9 show that RBD classification follows the visual trends for the extent of the disease in the three tested grape leaves. It is also visually apparent that the RBD areas show green pigmentation which is attributed to the green leaf as part of the RBD mapping. This suggests the possibility of mixed pixels around the neighborhood pixels of RBD that also possess some properties of both RBD and green leaf. Future studies include unmixing of these pixels and identifying thresholds where RBD can be detected even when the leaf visually shows green leaf coloration. This would be of value for early detection of the disease, if and when green leaf attributes visually dominate the mixed pixel.

During the supervised training of the SVM classifier, the user selected areas belonging to red blotch disease; however, differences in spectral response from such labeled spectra revealed that what was originally identified as RBD was in fact close, but different, in both pigmentation and texture on the leaf. The authors called these areas 'sunburn'. Sunburnt areas are differentiated here due to their different spectral signatures from that of red blotch diseased areas, which emphasizes the advantage of hyperspectral imaging over digital color photography or visual inspection alone which an untrained eye could easily miss.

5. CONCLUSIONS

Hyperspectral images of grape leaves have been acquired with SOC710-VP® visible-to-NIR range portable hyperspectral imaging camera with leaves on the vine, off-the-vine in the field, and after being returned to the lab. Using modified reflectance at two bands ($R_{566\ nm}$, $R_{628\ nm}$) and two modified reflectance ratios using four bands ($R_{566\ nm}$ / $R_{628\ nm}$, $R_{680\ nm}$ / $R_{738\ nm}$), red blotch disease is identifiable using hyperspectral imaging technology together with the discussed image processing and analysis techniques. Further studies involve quantification and monitoring of the progression of the disease for disease management and harvest planning in grape vines, and increasing the number of classes on the grape leaf area that are to be segmented using SVM classifier.

REFERENCES

[1] "Grapevine Red Blotch Disease," Fact Sheet, National Clean Plant Network, Brochure (February 2013). http://cemendocino.ucanr.edu/files/165430.pdf

[2] McFadden-Smith, W., "Grapevine red blotch associated virus: A newly identified disease in vineyards," Ontario Ministry of Agriculture, Food and Rural Affairs (15 August 2013). http://www.omafra.gov.on.ca/english/crops/hort/news/hortmatt/2013/22hrt13a1.htm

[3] Sudarshana, M. R., and Wolpert, J. A., "Grapevine Red Blotch Disease," United States Department of Agriculture Agricultural Research Service (November 2012). http://iv.ucdavis.edu/files/157508.pdf

[4] Rapaport, T., Hochberg, U. Shoshany, M.,Karnieli, A., and Rachmilevitch, S., "Combining leaf physiology, hyperspectral imaging and partial least squares-regression (PLS-R) for grapevine water status assessment," ISPRS Journal of Photogrammetry and Remote Sensing 109, 88-97 (2015).

[5] Fernandes, A. M., Melo-Pinto, P., Millan, B., Tardaguila, J., and Diago M. P., "Automatic discrimination of grapevine (*Vitis vinifera* L.) clones using leaf hyperspectral imaging and partial least squares," The Journal of Agricultural Science 153(03) 455-465 (2015).

[6] Lenk, S., Chaerle, L., Pfündel, E. E., Langsdorf, G., Hagenbeek, D., Lichtenthaler, H. K.., Van Der Straeten, D. and Buschmann, C., "Multispectral fluorescence and reflectance imaging at the leaf level and its possible applications," Journal of Experimental Botany 58(4) 807-814 (2007).

[7] Boser, B. E., Guyon, I. M., and Vapnik, V. N., "A training algorithm for optimal margin classifiers," Fifth Annual Workshop on Computational Learning Theory, ACM, 144–152 (June 1992)

[8] V. N. Vapnik, [Statistical Learning Theory], John-Wiley and Sons, Inc., New York (1998).

[9] Gualtieri, J. A. and Chettri, S., "Support vector machines for classification of hyperspectral data," IEEE International Symposium on Geoscience and Remote Sensing, 2, 813-815 (2000). 10.1109/IGARSS.2000.861712

[10] Garcia, J. and Barbedo, A., "Digital image processing techniques for detecting, quantiying and classifying plant diseases," SpringerPlus, 1-12 (2013). http://www.springerplus.com/content/2/1/660

[11] "SOC710-VP Hyperspectral Imager," Surface Optics Corp., https://surfaceoptics.com/products/hyperspectral-imaging/soc710-portable-hyperspectral-camera/ (March 31, 2016).

[12] Mehrubeoglu, M., Zemlan, M., and Henry, S., "Hyperspectral imaging for differentiation of foreign materials from pinto beans," Proc. SPIE 9611, Imaging Spectrometry, 96110A1-8 (2015). doi:10.1117/12.2207797